Water Science & Technology

IWA PUBLISHING

Water Science & Technology Vol 84 No 4, 995 doi: 10.2166/wst.2021.263

Phosphorus removal in domestic wastewater treatment plant by calcined eggshell

Rafael Renato Fritzen and Antônio Domingues Benetti*
Institute of Hydraulic Research, Federal University of Rio Grande do Sul, Bento Gonçalves Avenue, 9500, Agronomia, Porto Alegre, RS, Brazil
*Corresponding author. E-mail: benetti@iph.ufrgs.br

ADB, 0000-0002-5940-8866

ABSTRACT

Recovery of phosphorus (P) from wastewater is a topic of great interest. Besides being a non-renewable resource, P discharge in receiving waters can trigger algae blooms. The present study aimed to quantify the removal of P from two sites at a wastewater treatment plant using calcined eggshell (CES) as adsorbent. CES was prepared from raw shells calcined at 600 °C (CES600) and 800 °C (CES800). CES at 800 °C proved to be an efficient material for P removal. Efficiencies greater than 70% were achieved using CES800 concentrations of 0.1 g L^{-1} for synthetic sample, 0.3 g L^{-1} for preliminary treated wastewater and 20 g L^{-1} for supernatant from sludge anaerobic digester. The adsorption process was fast, occurring mostly in the first 30 min. Both Langmuir and Freundlich isotherms fitted the experimental data on adsorption. In kinetic experiments, a pseudo-second-order model fitted P adsorption from synthetic, preliminary effluent and digester supernatant. Thermogravimetric analysis showed a 54% eggshell mass loss at 800 °C. Calcination increased calcium and reduced carbon fractions in the eggshells, while increasing the surface area.

Key words: anaerobic digester supernatant, eggshell adsorbent, eggshell waste reuse, phosphorus adsorption, recycling wastewater nutrient

HIGHLIGHTS

- Calcined eggshells can remove phosphorus from wastewater.
- Eggshells calcined at 800 °C removed more than 70% of phosphorus.
- Most phosphorus adsorption took place in the first 30 min.
- The aggregate Ca–P has potential use in recycling valuable resources.

INTRODUCTION

The circular economy aims to keep the value of products, materials, and resources in the production process, minimizing the generation of waste. This approach seeks to separate economic development from the consumption of finite resources (Ellen MacArthur Foundation 2017). Various anthropogenic wastes and materials are integrated in this concept of circular economy.

Phosphorus (P) is an essential nutrient and is present in most fertilizers used in the global food production chain (Cordell *et al.* 2011; Wilfert *et al.* 2015). The main source of P is phosphate rocks, a non-renewable natural resource. The size of the world's phosphate reserves is a matter of divergence, with estimates of duration varying from decades to hundreds of years (Van Vuuren *et al.* 2010). However, there is general agreement that the quality of reserves is deteriorating in terms of content and quality (Desmidt *et al.* 2014), with extraction increasingly complex and costly. The production of phosphate rocks in 2018 was 270 million tons (US Geological Survey 2019).

Phosphorus is present in wastewater and is a pollutant when released into water bodies. It accelerates eutrophication, which can cause serious damage to aquatic ecosystems and water supply (Peng *et al.* 2018). Phosphorus concentration in domestic wastewater is in the range of 4–12 mg L^{-1} (Metcalf & Eddy 2014). Within wastewater treatment plants (WWTP), a major source of P is the supernatant of the anaerobic digestion of sludges formed in primary sedimentation tanks and biological treatment. This supernatant contains high concentrations of solids, biochemical oxygen demand (BOD) and nutrients,

and it is usually recycled to the head of the plant. P concentration in the supernatant of anaerobic digester varies in the range 110–470 mg/L (Metcalf & Eddy 2014).

Yuan *et al.* (2012) suggested that municipal wastewater is a potential source for P recycling and estimated that its recovery could satisfy 15% to 20% of world demand. One alternative for P recovery in wastewater and sludge treatment plants is its adsorption to a residue (Maroneze *et al.* 2014).

Eggs are one of the most important foods in the world, as they are sources of nutrients essential to human diet. According to the Brazilian Animal Protein Association (ABPA), in 2019 the national consumption of eggs was 230 units per person annually (ABPA 2020). The world production of eggs reached 7.2×10^7 t year^{-1} in 2017, representing an increase of 150% with respect to 1990 (FAO 2016). Eggshells are produced as waste when eggs are used directly for food or as raw material in the food industry. The shell represents approximately 11% of the egg's weight (Quina *et al.* 2017). Approximately 94% of the shell is composed of calcium carbonate (Mittal *et al.* 2016). Quina *et al.* (2017) classified the potential reuse of this material, including its use as food additive, soil correction, and as pollutant adsorbent (Figure 1).

Köse & Kivanç (2011) reported the use of calcined eggshell (CES) for adsorption of phosphate from aqueous solution. The authors found that desorption was not completely reversible. However, instead of recovering P to its natural form, an alternative is to use the resulting material (eggshell + P) as fertilizer.

Several studies using raw or modified calcined eggs have been reported. Morales-Figueroa *et al.* (2021) synthesized a material composed of eggshells, magnesium oxide and acetic acid. They found that total P could be eliminated from an industrial wastewater using 13.2 mg L^{-1} calcium magnesium acetate, pH 12 and 12 min contact time. Ribeiro *et al.* (2020) prepared an adsorbent using eggshell, hydrochloric acid and sodium hydroxide. The authors found that 329 mg P g^{-1} could be recovered using samples prepared from a P-stock solution. Using eggshell calcined at 800 °C, Torit & Phihusut (2018) measured 80% P removal from domestic wastewater containing 1.7 mg L^{-1} P. Almeida *et al.* (2020) produced adsorbents composed

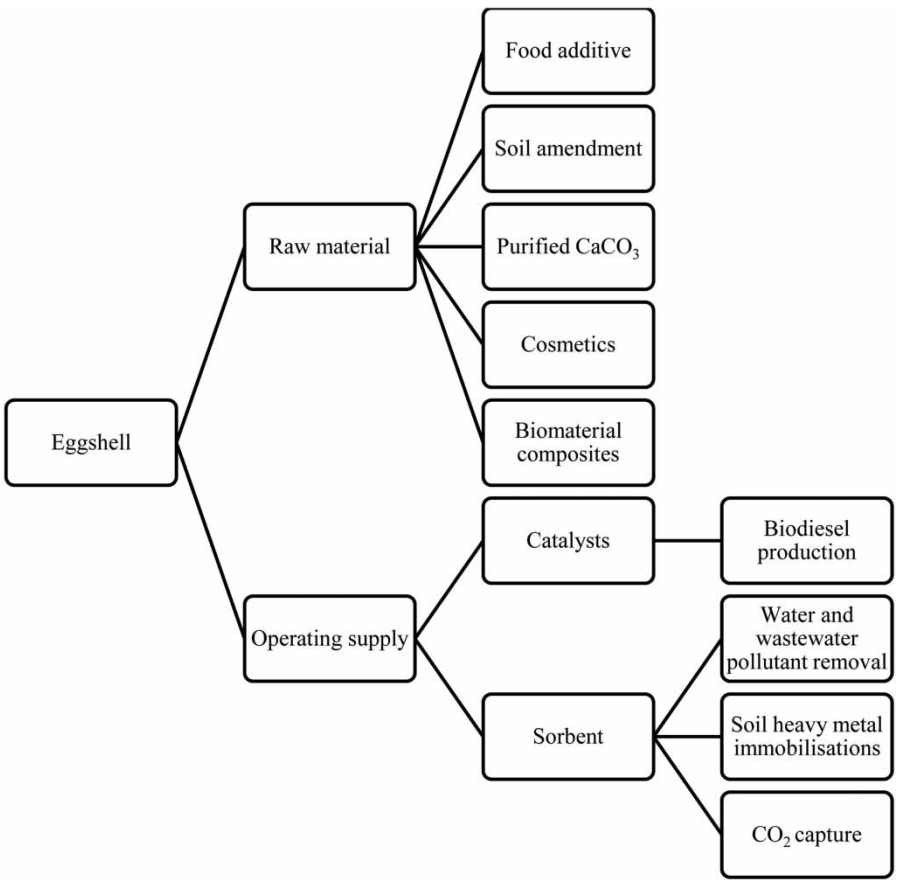

Figure 1 | Classification of potential uses for eggshell residues as raw material and operating supply. *Source*: Adapted (Quina *et al.* 2017).

of raw or CES modified by solutions of ferric chloride hexahydrate and magnesium chloride hexahydrate. The best adsorbent removed 99% P in samples prepared from stock solutions and 51.8% from an effluent containing 10 mg L^{-1} P. They concluded that the complex matrix of the effluent had a negative effect on adsorption. Panagiotou *et al.* (2018) used eggshells calcined at 900 °C for 30 min to adsorb P that was leached by sulfuric acid (H_2SO_4) from anaerobic digester sludge. The authors observed the formation of Brushite ($CaHPO_4{\cdot}2H_2O$), a material suitable to use as fertilizer.

This study aimed to evaluate the use of calcined and ground eggshells as adsorbent of P present in synthetic samples, in effluent from preliminary wastewater treatment, and in the supernatant of anaerobic digester used for sludge treatment. Eggshells were not modified other than calcination, and one focus of this work was the application of the adsorbent to the supernatant of anaerobic digester, a highly concentrated and complex liquid that is formed in wastewater treatment. It was hypothesized that a complex formed by Ca and P could be produced that has potential use as a soil conditioner in agriculture. However, this beneficial use was not tested in the present study.

METHODS

Materials

Eggshells were collected from household consumption of one of the authors. To remove impurities, the shells were rinsed with deionized water and subsequently dried at 100 °C for 24 h in an oven. After drying, the eggshells were separated into two parts. One was calcined in a furnace at 600 °C for 4 h, and the other at 800 °C for 2 h. The resulting products were named, respectively, CES600 and CES800. The CES were subsequently ground with a mortar and pestel. The resulting powder was screened through a sieve with size less than 0.595 mm (30 mesh). According to Panagiotou *et al.* (2018), CES with particle diameters less than 1 mm enhanced P adsorption capacity, since there was an increase in the specific surface area (SSA) of the material, as quantified through gas sorption data.

Preliminary tests were carried out with stock solutions composed of deionized water and monopotassium phosphate (KH_2PO_4), with P concentrations of 15 mg L^{-1} P. In addition, domestic wastewater samples were collected for adsorption and kinetics tests from an activated sludge municipal WWTP in Porto Alegre, Brazil. Samples from preliminary treatment effluent and supernatant from anaerobic digester were used for the tests. These sampling points were chosen due to the high concentrations of P present. All samples were collected on three different days. Table 1 shows preliminary treatment effluent and anaerobic digester supernatant composition of samples collected at the wastewater treatment plant. Parameters conductivity, total Kjeldahl nitrogen (TKN), total P, and alkalinity were more concentrated in supernatant than in preliminary effluent. In particular, the concentration of P was almost 19 times higher in supernatant, which makes this liquid attractive for P recovery techniques.

Table 1 | Preliminary treatment effluent and anaerobic digester supernatant composition (mean ± standard deviation) ($n = 3$)

Constituent	Unit	Preliminary treatment effluent	Anaerobic digester supernatant
Temperature	°C	22.6 ± 0.5	21.4 ± 0.4
pH	–	7.4 ± 0.2	7.5 ± 0.5
Conductivity	μS cm^{-1}	670 ± 68	3,670 ± 609
Turbidity	NTU	283 ± 288	114 ± 12
COD	mg O_2 L^{-1}	615 ± 303	313 ± 54
BOD_5^{20}	mg O_2 L^{-1}	305 ± 100	150 ± 52
BOD/COD	–	0.6 ± 0.2	0.5 ± 0.1
TKN	mg N L^{-1}	56 ± 26	430 ± 101
Total P	mg P L^{-1}	7.3 ± 2.9	137 ± 6
Alkalinity	mg $CaCO_3$ L^{-1}	240 ± 27	1,744 ± 392
TSS	mg L^{-1}	333 ± 318	176 ± 53

COD, chemical oxygen demand; BOD, biochemical oxygen demand, BOD_5^{20}, five-day biochemical oxygen demand at 20 °C, TSS, total suspended solids.

Adsorbent characterization

Thermogravimetry/derived thermogravimetry tests (TG/DTG), scanning electron microscopy (SEM), elemental composition, and SSA were used to characterize the adsorbents produced by eggshells (CES600 and CES800).

For the eggshell TG/DTG test, a term scale (SDT Q600, TA Instruments-Waters) was used. The test was carried out in nitrogen, using a heating ramp of 10 °C min^{-1}, at a temperature between 25 and 900 °C. SEM was performed with the Phenom ProX Desktop SEM equipment, operating in the range of 10 and 15 kV and nominal resolution of 8 nm. The microscope was equipped with an energy dispersive X-ray spectroscope, which allowed the chemical composition of CES600 and CES800 samples before and after the P adsorption tests to be determined. The SSA of the samples was examined using the nitrogen sorption method (Brunauer–Emmett–Teller (BET) method) using the equipment Micrometrics Tristar® II 3020.

Batch adsorption of phosphorus

A 100-mL stock solution with P concentration of 15 mg L^{-1} was added to 250-mL flasks containing 1–50 g L^{-1} of CES600 and 0.1–2 g L^{-1} of CES800. Isotherms tests were also made using preliminary treated effluent (7.3 ± 2.9 mg L^{-1} P) and anaerobic digester supernatant (137 ± 6 mg L^{-1} P). The flasks were placed in a shaking incubator (TE – 053, TECNAL) operating at 150 rpm and 20 °C. After 30 min of stirring, aliquots were taken from the flasks and separated by passing them through a 0.45 μm filter. The choice for 30 min contact time was based on a published article (Köse & Kivanç 2011) and preliminary adsorption tests. All experiments were conducted in triplicate, without pH control. The amount of P retained by unit mass of eggshell was calculated by Equation (1):

$$q_e = \frac{(C_o - C_e)\,V}{m} \tag{1}$$

where q_e is the mass of P adsorbed per unit mass of CES (mg g^{-1}); C_o and C_e are the initial and equilibrium P concentrations, respectively (mg L^{-1}); V is the volume of the solution (L); and m is the mass of CES added to the solution (g).

Langmuir and Freundlich models in their nonlinear form (Equations (2) and (3), respectively) were used to fit the adsorption of P (Metcalf & Eddy 2014).

$$q_e = q_{max} \times \frac{b \times C_e}{1 + b \times C_e} \tag{2}$$

$$q_e = k_f \times C_e^{\frac{1}{n}} \tag{3}$$

where q_e, and C_e were previously defined; q_{max} (mg g^{-1}) is the maximum adsorption capacity in the eggshell; b (L mg^{-1}) is the Langmuir constant; k_f is the Freundlich adsorption capacity parameter [(mg g^{-1})(L $mg^{-1})^{1/n}$]; and n is the Freundlich constant related to the adsorption capacity (mg g^{-1}) and adsorption intensity (L mg^{-1}).

Kinetic studies

Kinetic models are useful for understanding the dynamics of contaminant adsorption in the adsorbent, as well as the adsorption mechanism. Kinetic tests were performed using eggshell concentrations that showed the highest P removals. In these tests, the flasks were placed into a shaking table operating at 150 rpm and temperature of 20 °C. Aliquots were taken after contact times of 1, 5, 10, 15, 30, 45, 60, 90, and 120 min of agitation. The aliquots were filtered through 0.45 μm filters for P analysis. The adequacy of the results to the pseudo-first and second-order models was verified.

The pseudo-first and pseudo-second-order models are expressed, respectively, by Equations (4) and (5) (Lalley *et al.* 2016):

$$\log(q_e - q_t) = \log(q_e) - \frac{k_1}{2.303}t \tag{4}$$

$$\frac{t}{q_t} = \frac{1}{k_2 q_e^2} + \frac{t}{q_e} \tag{5}$$

where q_e and q_t are the amounts of P adsorbed (mg g^{-1}) at equilibrium time and any time t (min), respectively; k_1 is the rate constant of adsorption (1 min^{-1}); and k_2 is the pseudo-second-order rate constant (g mg^{-1} min^{-1}). The constants k_1, k_2, and the equilibrium adsorption capacity q_e were calculated from the nonlinear plot of q_t versus t.

Analytical techniques

Total P concentrations in samples were determined using the Stannous Chloride Method (4500-PD) (Standard Methods 2005). Absorbance was measured at 690 nm wavelength using spectrophotometer UV-1600, Pro-Analise. The samples collected at the WWTP were digested using the Persulfate Method (4500-PB.5) (Standard Methods 2005) to convert organic and acid-hydrolysable P to ortho-phosphate. Samples were not filtered before digestion. Other analysis made in wastewater and supernatant used standard methods from APHA (Standard Methods 2005): pH (method 4500–H^+ A), conductivity (method 2510 B), turbidity (nephelometry, method 2130 B), COD (closed reflux, titrimetric, Method 5220 C), 5-day BOD (respirometric, method 5210 D), TKN (Method 4500-N_{org} B), alkalinity (titration, method 2320 B), and TSS (gravimetric, method 2540 D).

Statistical analysis

The Wilcoxon–Mann–Whitney test was used to compare adsorption at temperatures 600 °C and 800 °C for each of the quantities of calcined eggs added. Analysis of variance (ANOVA) was used to compare removal means among the same sample. Two-way ANOVA was used to compare removal means and CES concentrations in raw, CES600, and CES800. The Tukey test was used for multiple comparisons for all possible pairs of CES800 eggshell concentrations. All tests considered a significance level of 0.05. The correlation between pH and P removal was determined with the Spearman coefficent. R software from RSudio plataform was used for statistical analysis. Nonlinear regression models were calculated using Excel software.

RESULTS AND DISCUSSION

Eggshell characterization

The TG/DTG curve of the eggshell thermal decomposition reaction is shown in Figure 2. The data showed that the thermal decomposition of the eggshell could be divided into three events of mass losses. The first ($\Delta m_1 = 2.7\%$), which occurred between 25 °C and 100 °C, can be attributed to the loss of moisture in the eggshell. The second event occurred between 100 °C and 600 °C, with mass loss Δm_2 equal to 15.1%. Decomposition of organic matter took place in this range of temperature. The greatest reduction in eggshell mass happened between 600 °C and 765 °C, with mass loss Δm_3 of 35.8%. Higher

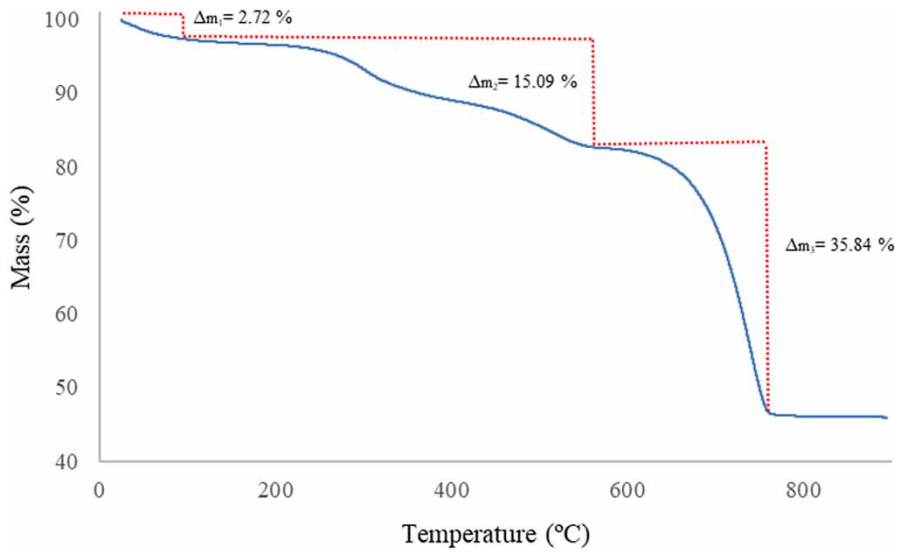

Figure 2 | Thermogravimetric curve relating the percentage of remaining eggshell mass and percentage remaining per unit temperature ($\beta = 10$ °C min^{-1} between 25 and 900 °C). Legend: Δm_i = mass variation (%) for temperature variation Δt_i; blue line = thermal decomposition of the eggshell. Please refer to the online version of this paper to see this figure in colour: http://dx.doi.org/10.2166/wst.2021.263.

temperatures promote the release of carbon dioxide (CO_2) and calcium oxide (CaO) formation. Upon reaching 900 °C, there was a total loss of mass of 54%. Rodrigues & Ávila (2017) found reductions of 1.0%, 7.7% and 39.5% for Δm_1, Δm_2 and Δm_3.

The SSA of the eggshell particles were measured by the nitrogen sorption method (BET method). The gas sorption measurements indicated that SSA increased as the calcination temperature rose. The raw eggshells (ES), CES600 and CES800 presented SSA of 0.30 $m^2 g^{-1}$, 0.65 $m^2 g^{-1}$ and 2.8 $m^2 g^{-1}$, respectively. CES800 surface area increased 4.3 times in relation to CES600 and 9.4 times in relation to ES. Panagiotou *et al.* (2018) reported SSA for ES, CES600, CES800, and CES900 of 0.31 $m^2 g^{-1}$, 0.41 $m^2 g^{-1}$, 1.3 $m^2 g^{-1}$ and 1.6 $m^2 g^{-1}$, respectively.

Figure 3 shows an illustration of raw ground eggshells and those that have been calcined at 600 °C for 4 h and 800 °C for 2 h. The increase in calcination temperature resulted in residues with different visual characteristics, such as size and color of particles.

The eggshell has a porous structure, responsible for the gas exchange between the external and internal media. Figure 4 shows SEM images of CES600 and CES800 in different magnifications (×500, ×1,000, and ×2,000). The images indicated that the increase in temperature resulted in greater porosity of the residues, corroborating the results of the BET analyses.

In addition to morphological changes that were induced by the increase in the calcination temperature, there were also chemical changes. Table 2 shows the elemental composition of ES, CES600, and CES800, as quantified by means of a characteristic X-ray detector. As the calcination temperature increased, the atomic carbon (C) concentration decreased while calcium (Ca) increased. The increase in Ca concentration was associated with a decrease in the relationship between carbon and oxygen (C/O) from 1.00 (ES) to 0.52 (CES800). Higher calcination temperatures cause the conversion of calcium carbonate to calcium oxide (CaO) according to Equation (6). It indicates that the mass of Ca remains constant while carbon decreases through transformation into gas.

$$CaCO_3 \rightarrow CaO + CO_2 \quad (6)$$

After carrying out the adsorption tests, the CES800 adsorbents were again visualized with SEM (Figure 5) and had chemical composition measured by energy dispersive X-ray spectroscopy. Table 3 shows the elemental compositions of the CES800 adsorbent after the adsorption test with the supernatant of the anaerobic digester. The CES800 composition remained similar as before adsorption. The evidence that P was not found as a major element in the composition of CES800 after the adsorption test may be related to the fact that its increase was not sufficient to represent a significant fraction of the adsorbent material.

Phosphorus removal

Figure 6 presents the results of the P removal tests with different concentrations of eggshell applied to samples from synthetic and preliminary treatment effluent with CES600 (a), with CES800 (b), and sample from the anaerobic digester supernatant, using CES800 (c).

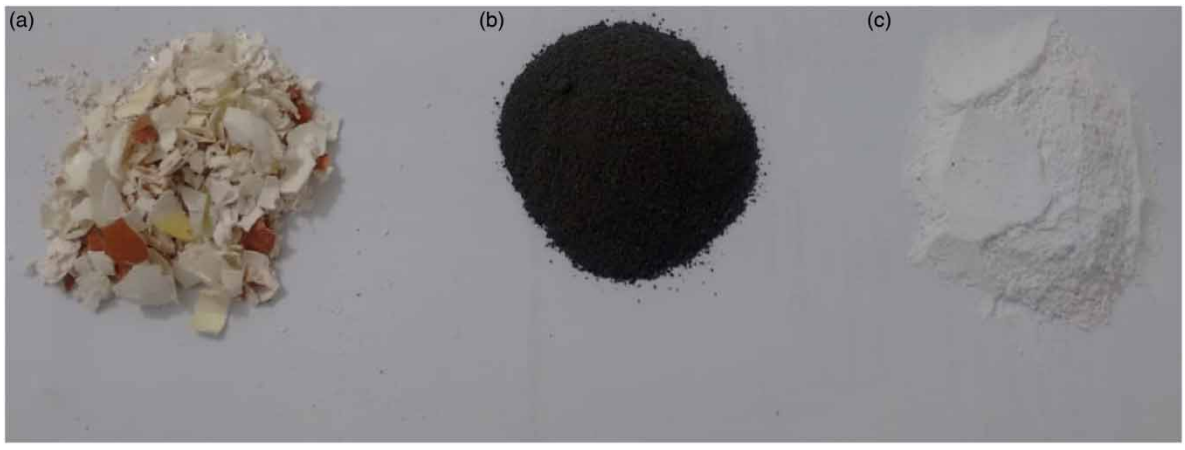

Figure 3 | Illustrations of (a) raw eggshell (ES), (b) eggshell calcined at 600 °C for 4 h (CES600), (c) eggshell calcinated at 800 °C for 2 h (CES800).

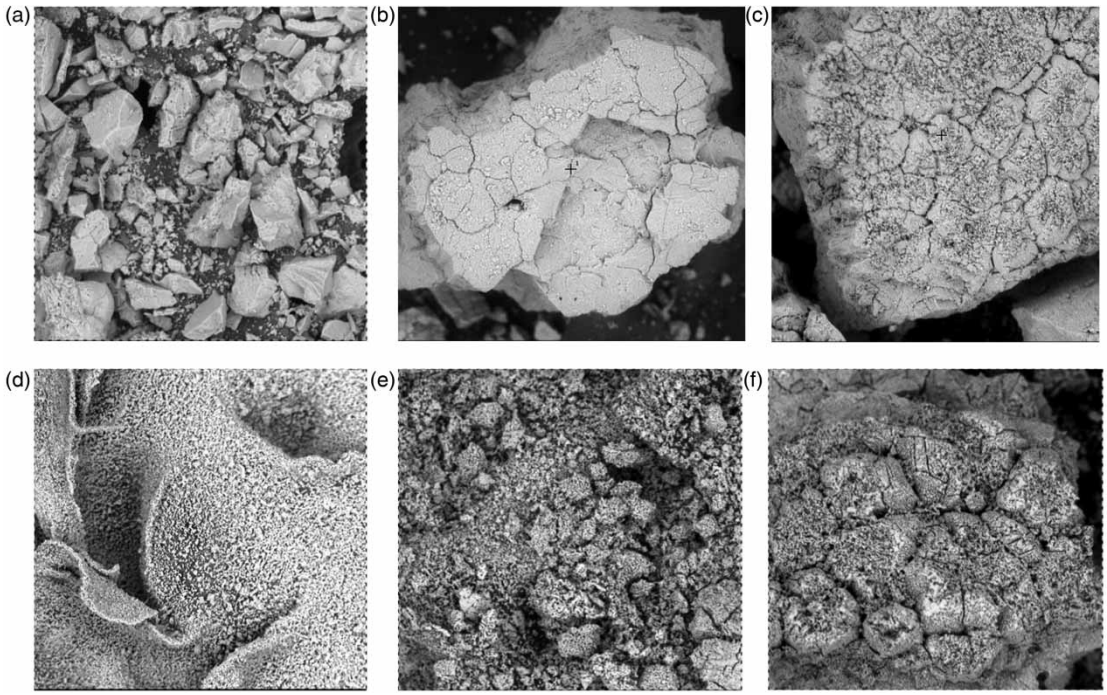

Figure 4 | SEM images of CES600 (a)–(c) and CES800 (d)–(f). From left to right, the magnifications are ×500, ×1,000, and ×2,000, respectively. All images were taken before adsorption tests.

Table 2 | Elemental composition of ES, CES600, and CES800 as quantified through energy dispersive X-ray spectroscopy

Element	ES Atomic concentration (%)	CES600 Atomic concentration (%)	CES800 Atomic concentration (%)
O	46.7	51.0	46.1
C	47.0	28.5	24.0
Ca	6.2	18.3	26.8
Other elements: Na, K, Mn, Fe, Cu, Sr	0.15	2.2	3.1

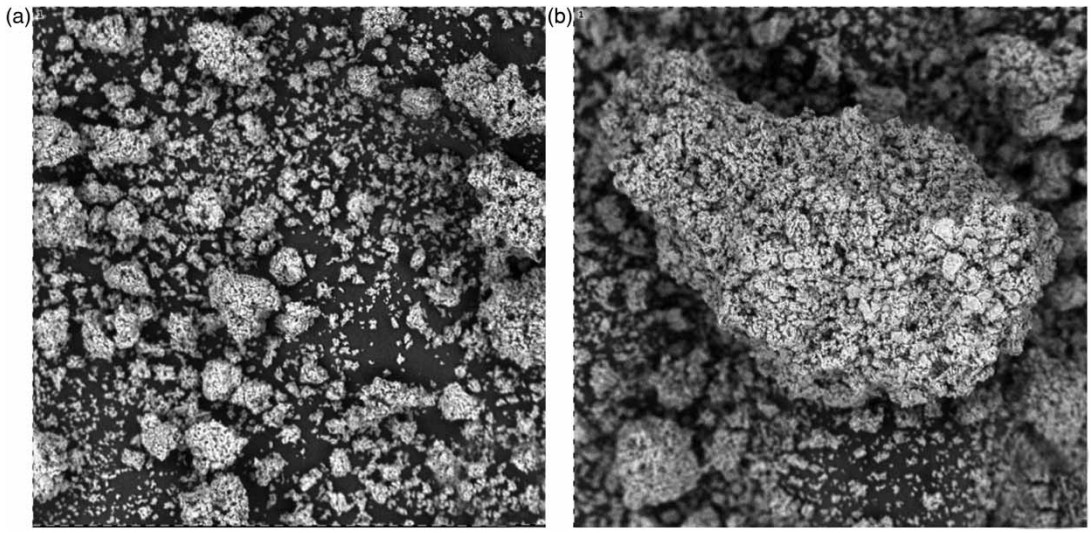

Figure 5 | SEM images of CES800 after the second adsorption test with supernatant from sludge anaerobic digester. Magnifications are (a) ×1,000 (b) ×2,000.

Table 3 | Elemental composition of CES800 after adsorption test with supernatant of the anaerobic digester

Element	CES800 after adsorption test with supernatant from anaerobic digester Atomic concentration (%)
O	43.6
C	27.0
Ca	26.1
Other elements: Na, K, Mn, Fe, Cu, Sr	3.3

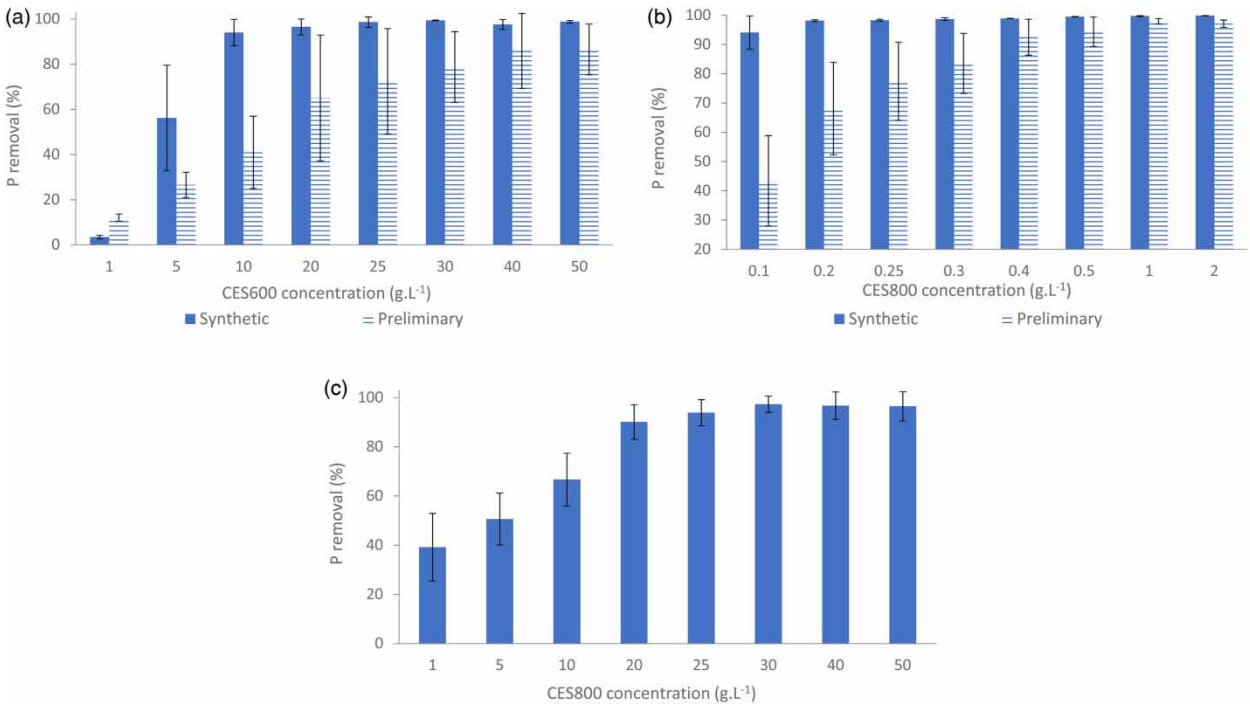

Figure 6 | Phosphorus removal in synthetic samples and preliminary treatment effluent samples with different concentrations of CES600 (a), CES800 (b), and CES800 for samples from the anaerobic digester supernatant (c). Contact time 30 min and number of samples ($n = 3$).

The results show that for CES600 the efficiency of P removal varied according to the sample. For the synthetic solution, which had an initial P concentration of 15 mg L^{-1} P, 10 g L^{-1} CES600 removed more than 90% of P. In preliminary treated effluent, this removal could not be reached even using a concentration five times as high. For the preliminary treated effluent, the removal efficiency grew with increasing adsorbent concentration, reaching up to 85% removal. Almeida *et al.* (2020) observed P removal decreased from 99% in stock solutions to 51.5% in wastewater effluent. They attributed the reduction to the complex nature of the effluent in comparison to the stock solutions.

The eggshell concentrations of the CES800 adsorbent were 10–25 times lower than the concentrations that were used with CES600 (Figure 6(a) and 6(b)). A CES800 concentration of just 0.1 g L^{-1} was sufficient to remove more than 90% of P in the synthetic sample. For the preliminary effluent, 1.0 g L^{-1} CES800 removed 98% P. At a significance level of 0.05, application of Wilcoxon–Mann–Whitney test rejected the null hypothesis of equality in the efficiency of P removal by eggshells calcined at temperatures 600 °C and 800 °C ($p < 0.001$).

Application of the Tukey test for comparisons of all possible pairs of CES800 eggshell concentrations showed there were no significant differences in P removal for CES800 concentrations higher than 0.1 g L^{-1} in synthetic solution. For P adsorption

from preliminary effluent, CES800 concentrations above 0.3 g L^{-1} were not significant. Therefore, the concentration of 0.3 g^{-1} could be chosen to remove 85% of the initial concentration of P with 30 min contact time.

The initial P concentration in the supernatant from anaerobic digester was 137 ± 6 mg L^{-1}, which was higher than those in the other samples. For this reason, concentrations of CES800 had to be much higher than those used for synthetic and preliminary effluent samples. For instance, the application 1.0 g L^{-1} of CES800 removed more than 95% of P in preliminary effluent (Figure 6(b)), but only 39% in supernatant (Figure 6(c)). To achieve 95% P removal from supernatant, a CES800 concentration of 30 g L^{-1} was needed.

ANOVA was used to verify whether there were significant differences in the percentages of P removal from the supernatant of the digester with respect to the increase in the concentration of CES800 eggshell. For significance level of 0.05, the hypothesis that there were no differences between the concentrations of CES800 used for P removal was rejected ($p < 0.05$). The results of application of the Tukey test for comparisons of all possible pairs of CES800 eggshell concentrations are shown in Figure 7. All comparisons of CES800 eggshells concentrations that were significantly different are shown in blue. The pairs of concentrations that were not significantly different cross the zero value in the estimated range, and are shown in red. The only pairs of concentrations that were not significantly different were those involving concentrations higher than 20 g L^{-1}. At this concentration, CES800 removed 90% of the initial concentration of P with a contact time of 30 min.

pH effect

Figure 8 shows the pH values measured in anaerobic digester supernatant after 30 min contact time for different CES800 concentrations. The initial pH of the supernatant was approximately 7.5 and gradually increased as the adsorbent concentration increased. With CES800, a concentration 50 times greater than used in preliminary effluent was required to reach pH 12. This behavior was due to the buffer capacity of the supernatant that resulted from the production of bicarbonate during decomposition of proteins in anaerobic digestion.

Correlation analysis was used to assess the relationship between pH and P removal. The non-parametric Spearmans coefficient was 0.92, indicating a strong correlation. Figure 9 shows the fraction of P removed as function of pH. Above pH 11, P removal was over 90%. A possible explanation for the correlation between pH and P removal is the reaction between Ca and P, with formation of hydroxyapatite (Metcalf & Eddy 2014). CaO is more soluble than $CaCO_3$, and, in solution, can lead to

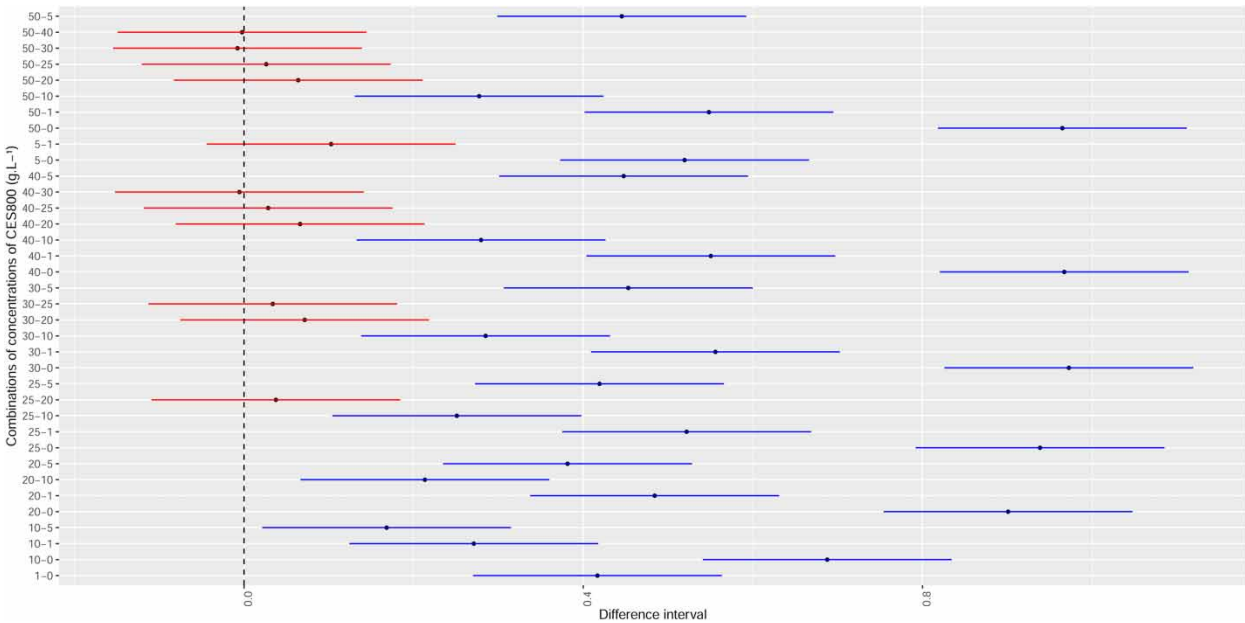

Figure 7 | Tukey test for multiple comparisons for all possible pairs of CES800 concentrations applied to the anaerobic digester supernatant. Red lines = not significant differences between CES concentration pairs; blue lines = significant differences between CES concentration pairs. Please refer to the online version of this paper to see this figure in colour: http://dx.doi.org/10.2166/wst.2021.263.

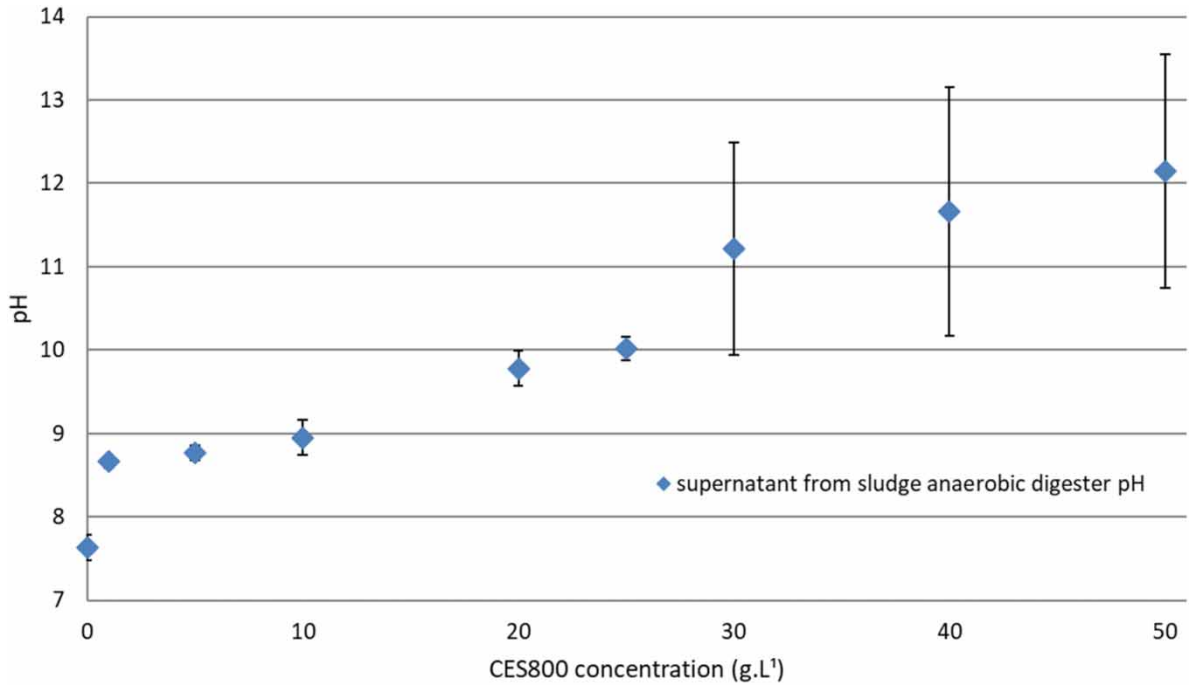

Figure 8 | pH values relative to CES800 concentrations in contact with anaerobic digester supernatant after 30 min contact time (means ± standard deviations).

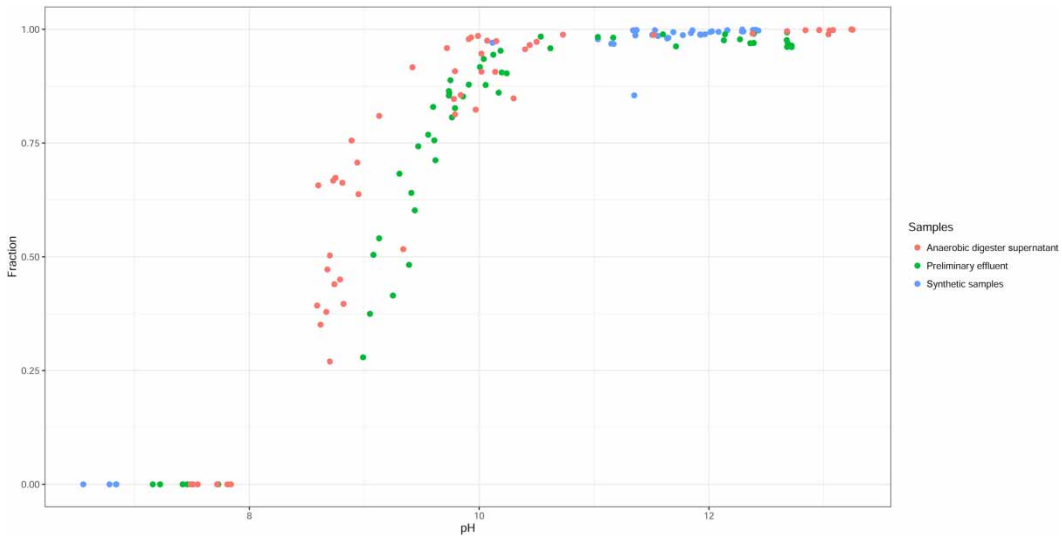

Figure 9 | Fraction of P removed relative to pH in synthetic, preliminary effluent, and digester supernatant samples.

precipitation of calcium phosphate ($Ca_3(PO_4)_2$) (Molle *et al.* 2005; Paradelo *et al.* 2016). However, these results cannot be understood only because of the pH increase because higher pH values were reached using higher eggshell concentrations and therefore had larger surface areas available for P adsorption.

Köse & Kivanç (2011) measured positive values of zeta potential on the surface of CES in the pH range 2–10. Because of the positive charge in eggshell surface and the negative charge of phosphate ions, these authors considered electrostatic attraction an

important mechanism of P removal. They found that more than 99% P removal could be reached in the pH range 2–10. This was different from what was measured in the present study, as shown in Figure 9, with maximum removal at pH above 10.

The solubility between solid $Ca_3(PO_4)_2$(s) and liquid phases (Ca^{+2} and PO_4^{3-}) is affect by the ionic strength (μ) of the solution. Electrical conductivity (EC) and μ are related, and Equation (7) can be used for an estimation of μ (Snoeyink & Jenkins 1980).

$$\mu = 1.6 \times 10^{-5} \times EC \tag{7}$$

where EC is the electrical conductivity of the solution (μS cm^{-1}).

Based on values of EC presented in Table 1, μ of preliminary effluent and digester supernatant were 0.011 and 0.059, respectively. Because of its much higher ionic strength, the adjusted equilibrium solubility product constant in digester supernatant was approximately 4.5 times lower than in preliminary effluent. Both samples had lower solubility constants than in solutions with ideal behavior, in which molar concentrations were used. Estimations of the adjusted solubility product constants for preliminary effluent and digester supernatant is presented in the Supplementary Material.

Adsorption isotherms

The nonlinear equations of Langmuir and Freundlich models were applied to adsorption of P present in synthetic water, preliminary treated effluent, and supernatant from anaerobic digester. For the latter, only CES800 was used considering previous results showing that this adsorbent needed much lower concentrations than CES600. The Langmuir isotherm model assumes a homogeneous surface with a fixed number of accessible sites for adsorption, all with the same activation energy and reversible chemical equilibrium. The Freundlich equilibrium model is suitable for heterogeneous surfaces (Nazaroff & Alvarez-Cohen 2001).

The Langmuir (q_{max}, b) and Freundlich (k_f, $1/n$) constants are presented in Tables 4 and 5, together with the coefficients of determinations R^2 and the normalized mean square error (NMSE). Lower NMSE values describe a better fit (Foo & Hameed 2010). The experimental data and model for CES600 and CES800 are shown in Figure 10.

Table 4 | Langmuir model parameters for P removal in synthetic, preliminary effluent, and supernatant from anaerobic digester

		Langmuir (constants)			
Samples	**Isotherms**	**q_{max}**	**b**	**R^2**	**NMSE**
Synthetic samples	CES600	1.9	1.3	0.97	0.0681
	CES800	263	1.3	0.83	0.0092
Preliminary effluent	CES600	0.55	0.32	0.92	0.0065
	CES800	36	1.3	0.98	0.0071
Anaerobic digester supernatant	CES800	1.6	0.05	0.90	0.0371

Table 5 | Freundlich model parameters for P removal in synthetic, preliminary effluent, and supernatant from anaerobic digester

		Freundlich (constants)			
Samples	**Isotherms**	**k_f**	**$\frac{1}{n}$**	**R^2**	**NMSE**
Synthetic samples	CES600	0.87	0.40	0.67	0.1152
	CES800	161	0.73	0.97	0.1139
Preliminary effluent	CES600	0.14	0.57	0.96	0.0042
	CES800	18	0.42	0.95	0.0055
Anaerobic digester supernatant	CES800	0.18	0.46	0.88	0.0221

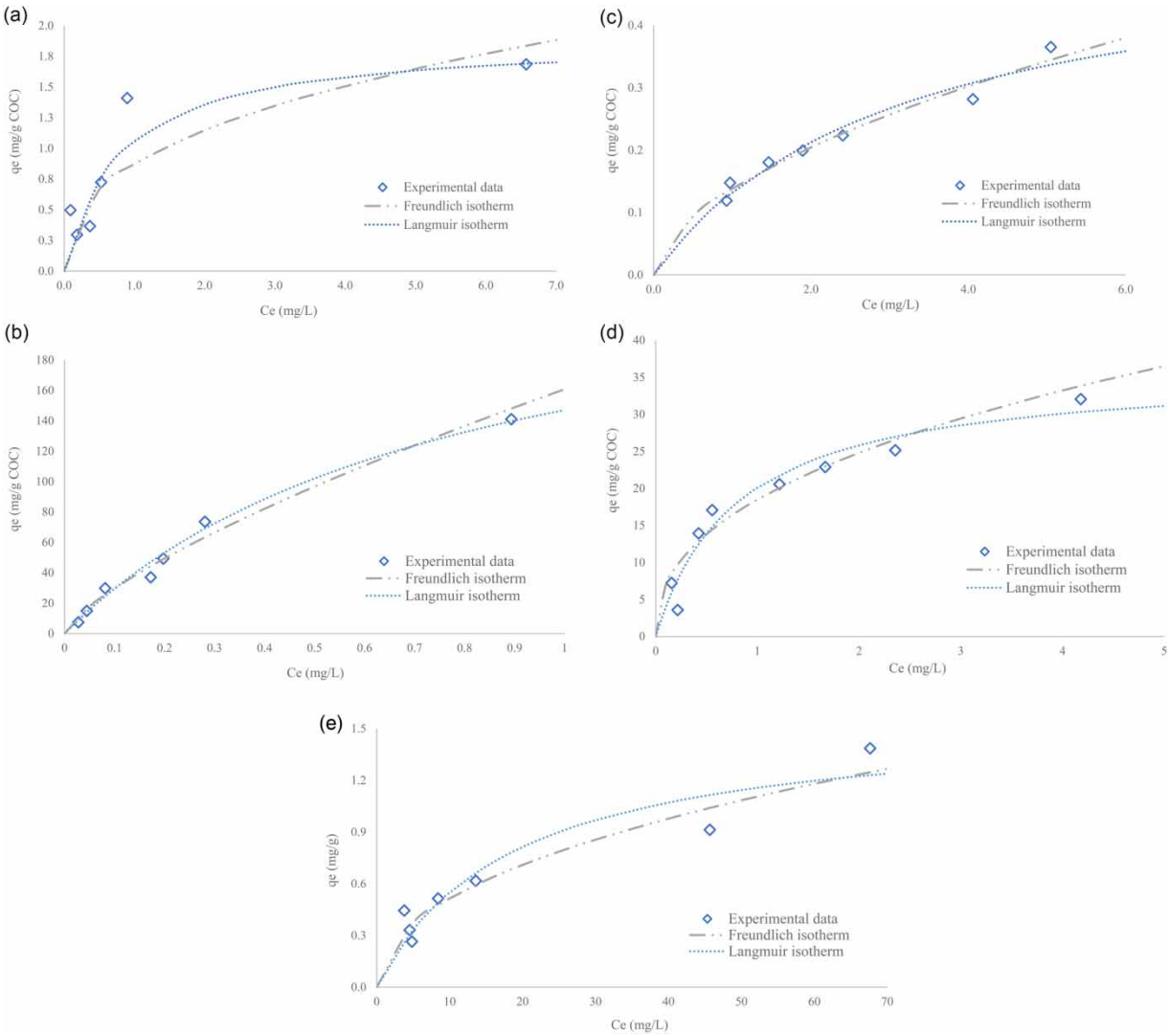

Figure 10 | Experimental data and fitted nonlinear adsorption isotherms (Langmuir and Freundlich) for (a) CES600 and (b) CES800 in synthetic samples at initial P concentration of 15 mg L^{-1}; (c) CES600 and (d) CES800 in preliminary treated wastewater with initial P concentration of 7.3 $\pm$ 2.9 mg L^{-1}P, (e) CES800 adsorbent in anaerobic digester supernatant with initial P concentration of 137 $\pm$ 6 mg·L^{-1} P.

Table 6 | Adsorption capacities reported for CES and other adsorbents

References	Adsorption capacity (mg g^{-1})	Sample	Calcination temperature (°C)
Molle *et al.* (2005)	4.76	P diluted in distilled water (1,000 µS cm^{-1})	Apatite
Mezenner & Bensmaili (2009)	10.60	P diluted in distilled water	Iron hydroxide eggshell
Köse & Kivanç (2011)	23.02	P diluted in distilled water	Eggshell at 800 °C for 2 h
Paradelo *et al.* (2016)	18.23	P diluted in distilled water (0.01 M $NaNO_3$)	Grounded mussel shell
	38.75	P diluted in distilled water (0.01 M $NaNO_3$)	Mussel shell 550 °C for 15 min
Panagiotou *et al.* (2018)	7.94	P diluted in distilled water	Eggshell at 800 °C for 2 h
	31.74	P diluted in distilled water	Eggshell at 900 °C for 30 min
Torit & Phihusut (2018)	121.00	P diluted in distilled water	Eggshell at 800 °C for 2 h
Ribeiro *et al.* (2020)	328.90	P diluted in distilled water	Hydroxyl eggshell
This study	263	P diluted in distilled water	Eggshell at 800 °C for 2 h
	36	Preliminary treatment effluent	Eggshell at 800 °C for 2 h
	1.6	Anaerobic digester supernatant	Eggshell at 800 °C for 2 h

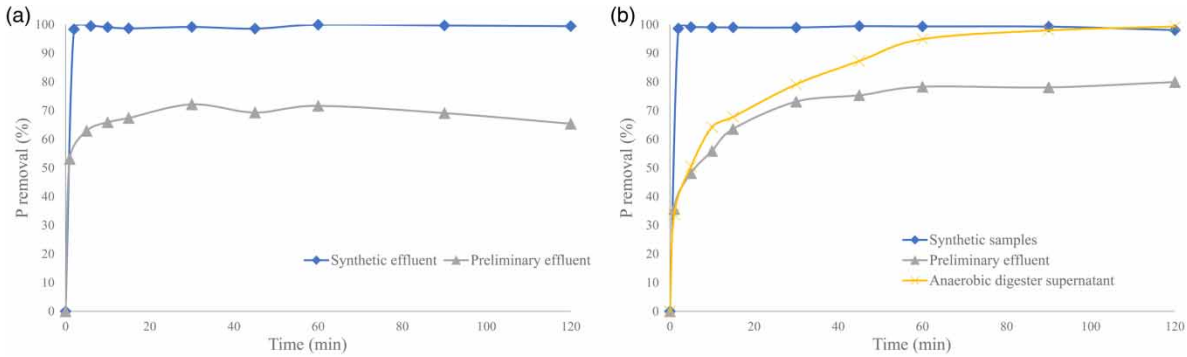

Figure 11 | Kinetic tests with synthetic, preliminary effluent, and anaerobic digester supernatant samples: (a) CES600 and (b) CES800. Concentrations of 0.1 g L^{-1} for the synthetic sample, 0.3 g L^{-1} for the preliminary effluent, and 20 g L^{-1} for the anaerobic digester supernatant.

Both models fitted relatively well experimental data. Phosphorus removal is normally described as adsorption on a heterogeneous surface, as the Freundlich model (Köse & Kivanç 2011). On the other hand, Panagiotou *et al.* (2018) found that the Langmuir model described better P adsorption to CES.

The adsorption capacities q_{max} in Langmuir equation were 263, 36, and 1.6 mg P g^{-1} CES800, respectively, for synthetic sample, preliminary treatment effluent, and digester supernatant. The adsorption capacity depended on the sample, and was higher for stock solution and lower in digester supernatant. Complex samples have more chemicals constituents competing for the adsorption sites (Benjamin & Lawler 2013). The lower q_{max} indicated there were less sites available for P adsorption compared with synthetic and preliminary effluent samples.

Table 6 shows maximum adsorption capacities for CES and other adsorbents reported in other studies. Except for this study, all isotherm tests were made using P diluted in distilled water, which may not represent adsorption in complex liquids. Adsorption capacities varied 69 times from lower to higher values of q_{max}. The adsorption capacity of CES800 for P in anaerobic digester supernatant was much lower than those for samples prepared from distilled water.

Kinectic studies

Kinetic tests were carried out to analyze the behavior of P adsorption by the adsorbent over time. A 20 g L^{-1} CES600 concentration was used for tests with synthetic and preliminary effluent samples. For the CES800 adsorbent, the concentrations used were 0.1 g L^{-1} for the synthetic sample, 0.2 g L^{-1} for the preliminary effluent, and 20 g L^{-1} for supernatant from the anaerobic digester. These concentrations were chosen for P removal efficiencies above 70%. The tests lasted 120 min. Samples were collected during the testing period. Figure 11 shows the results from the tests.

Phosphorus removal was fast in the synthetic sample, reaching almost 100% in less than 5 min. In preliminary treated effluent, removal reached 70% with CES600 and 80% with CES800. Most of the adsorption occurred within 30 min. Köse & Kivanç (2011) and Panagiotou *et al.* (2018) tested adsorption to CES over 10 h and 24 h, and found that most of the adsorption took place in the first 30 min.

It is interesting to note that removal of P from the digester supernatant was higher than in effluent from preliminary treatment, reaching almost 100% after 90 min. P concentration in supernatant was about 19 times higher than in the effluent (137 versus 7.3 mg L^{-1} P) and this might have improved the adsorption to CES800 adsorbent. Eggshell concentration for digester supernatant was 100 times the concentration used in preliminary effluent. Calcium released into solution from CES could have reacted with phosphate ions to form precipitates as discussed earlier.

The parameters calculated for the pseudo-first and second-order kinetics models are shown in Tables 7 and 8, respectively, together with the values of R^2 and NMSE. For synthetic sample and preliminary effluent, the results showed that the pseudo-second-order model represented the experimental data better compared to the pseudo-first-order model. For supernatant of anaerobic digester, both models fitted the data well. These results support findings from previous studies on the adsorption of P (Köse & Kivanç 2011; Oliveira *et al.* 2015; Panagiotou *et al.* 2018).

Table 7 | Kinetic constants of the pseudo-first-order model, determination coefficients, and NMSE for P removal in synthetic, preliminary effluent, and digester supernatant samples

			Pseudo-first-order		
Sample	**Adsorbent**	**Concentration (g L^{-1})**	**k_1**	**R^2**	**NMSE**
Synthetic	CES600	20	$2.4 \cdot 10^{-2}$	0.345	0.734
	CES800	0.1	$6.5 \cdot 10^{-3}$	0.477	3.007
Preliminary effluent	CES600	20	$3.5 \cdot 10^{-3}$	0.398	3.544
	CES800	0.2	$8.8 \cdot 10^{-3}$	0.733	0.921
Anaerobic digester supernatant	CES800	20	$3.8 \cdot 10^{-2}$	0.995	0.099

Table 8 | Kinetic constants of the pseudo-second-order model, determination coefficients, and NMSE for P removal in synthetic, preliminary effluent, and digester supernatant samples

			Pseudo-second-order		
Sample	**Adsorbent**	**Concentration (g.L^{-1})**	**k_2**	**R^2**	**NMSE**
Synthetic	CES600	20	17	1	0.000
	CES800	0.1	0.22	1	0.000
Preliminary effluent	CES600	20	18	0.902	0.151
	CES800	0.2	$3.4 \cdot 10^{-3}$	0.975	0.033
Anaerobic digester supernatant	CES800	20	$2.0 \cdot 10^{-2}$	0.999	0.021

CONCLUSIONS

Adsorbent produced by eggshell calcined at 800 °C for 2 h was able to remove P in samples from wastewater. At concentrations of 0.3 g L^{-1} and 20 g L^{-1}, CES800 removed more than 70% of the P present in preliminary effluent and supernatant from anaerobic digester after 30 min contact time.

The thermal decomposition of the eggshell was divided into three mass loss events, totaling 54% loss at 800 °C. Also, at this temperature of calcination, the SSA of the eggshell increased by 4.3 times the area formed at a temperature of 600 °C and 9.3 times the area of the raw eggshell.

In addition to morphological changes that were induced by the increase in the calcination temperature, there were also chemical changes. With higher calcination temperatures, atomic calcium concentration increased, and carbon decreased. The elementary compositions of the adsorbents before and after the contact times with samples were similar.

Langmuir and Freundlich isotherm models fitted the experimental data well. There was a clear effect of pH on the removal process. $Ca_3(PO_4)_2$ precipitation was a potential secondary mechanism for P removal, in addition to the adsorption process. The kinetics of P adsorption was fast, occurring especially during the first 30 min. The pseudo-second-order model fitted the experimental data better, although the first-order model was also a good fit for P adsorption from the supernatant of digester.

It is possible to expand the tests with CES800 for continuous and mixed flow reactors considering the excellent removal that was achieved in 30 min of contact time. Further studies can advance knowledge about the potential use of the eggshell–P aggregate in agriculture as a soil conditioner, reusing a non-renewable resource (P) and a reusable waste (eggshells), which is usually sent to landfills. An economic feasibility evaluation for producing the adsorbent is also required.

DATA AVAILABILITY STATEMENT

All relevant data are included in the paper or its Supplementary Information.

REFERENCES

Almeida, P. V., Santos, A. F., Lopes, D. V. & Gando-Ferreira, L. M. 2020 Novel adsorbents based on eggshell functionalized with iron oxyhydroxide for phosphorus removal from liquid effluents. *Journal of Water Process Engineering* **36**, 101248. https://doi.org/10.1016/j.jwpe.2020.101248

APHA, AWWA & WEF 2005 *Standard Methods for the Examination of Water and Wastewater*, 21st edn. American Public Health Association (APHA)/American Water Works Association (AWWA)/Water Environment Federation (WEF), Washington, DC, USA.

Associação Brasileira de Proteína Animal (ABPA) 2020 *Relatório Anual 2019 (Animal Protein Brazilian Association. 2019 Annual Report)*. São Paulo, Brazil. Available from: https://abpa-br.org/wp-content/uploads/2019/08/Relat%C3%B3rio-Anual-2019.pdf (accessed 10 October 2020).

Benjamin, M. M. & Lawler, D. F. 2013 *Water Quality Engineering*. Wiley, Hoboken, NJ.

Cordell, D., Rosemarin, A., Schröder, J. J. & Smit, A. L. 2011 Towards global phosphorus security: a systems framework for phosphorus recovery and reuse options. *Chemosphere* **84** (6), 747–758. doi:10.1016/j.chemosphere.2011.02.032.

Desmidt, E., Ghyselbrecht, K., Zhang, Y., Pinoy, L., Van der Bruggen, B., Verstraete, W., Rabaey, K. & Meesschaert, B. 2014 Global phosphorus scarcity and full-scale P-recovery techniques: a review. *Critical Reviews in Environmental Science and Technology* **45** (4), 336–384. doi: 10.1080/10643389.2013.866531.

Ellen MacArthur Foudation 2017 *A Circular Economy in Brazil: An Initial Exploration*. São Paulo, Brazil. Available from: https://www.ellenmacarthurfoundation.org/assets/downloads/A-Circular-Economy-in-Brazil-An-initial-exploration.pdf (accessed 20 November 2020).

Foo, K. Y. & Hameed, B. H. 2010 Insights into the modeling of adsorption isotherm systems. *Chemical Engineering Journal* **156** (1), 2–10. doi:10.1016/j.cej.2009.09.013.

Food and Agriculture Organization of the United Nations 2016 *World Production of Eggs*. Available from: http://www.fao.org/home/en/ (accessed 25 August 2020).

Köse, T. E. & Kivanç, B. 2011 Adsorption of phosphate from aqueous solutions using calcined waste eggshell. *Chemical Engineering Journal* **178** (15), 34–39. https://doi.org/10.1016/j.cej.2011.09.129

Lalley, J., Han, C., Li, X., Dionysiou, D. & Nadagouda, M. 2016 Phosphate adsorption using modified iron oxide-based sorbents in lake water: kinetics, equilibrium, and column tests. *Chemical Engineering Journal* **284**, 1386–1396. https://doi.org/10.1016/j.cej.2015.08.114

Maroneze, M. M., Zepka, L. Q., Vieira, J. G., Queiroz, M. I. & Jacob-Lopes, E. 2014 A tecnologia de remoção de fósforo: gerenciamento do elemento em resíduos industriais. (Phosphorus removal technology: managing the element in industrial residues). *Revista Ambiente e Água* **9** (3), 445–458. https://doi.org/10.4136/ambi-agua.1403

Metcalf & Eddy 2014 *Wastewater Engineering: Treatment and Resource Recovery*, 5th edn. McGraw-Hill, New York.

Mezenner, N. Y. & Bensmaili, A. 2009 Kynetics and thermodynamic study of phosphate adsorption on iron hydroxide-eggshell waste. *Chemical Engineering Journal* **147**, 87–96. doi:10.1016/j.cej.2008.06.024.

Mittal, A., Teotia, M., Soni, R. K. & Mittal, J. 2016 Applications of egg shell and egg shell membrane as adsorbents: a review. *Journal of Molecular Liquids* **223**, 376–387. https://doi.org/10.1016/j.molliq.2016.08.065

Molle, P., Lienard, A., Grasmick, A., Iwema, A. & Kabbabi, A. 2005 Apatite as an interesting seed to remove phosphorus from wastewater in constructed wetlands. *Water Science and Technology* **51** (9), 193–203. doi: 10.2166/wst.2005.0318.

Morales-Figueroa, C., Teuti-Sequeira, A., Linares-Hernández, I., Martínez-Miranda, V., Garduño-Pinedo, L., Barrera-Díaz, C. E., García-Morales, M. A. & Mier-Quiroga, M. A. 2021 Phosphate removal from food industry wastewater by chemical precipitation treatment with biocalcium eggshell. *Journal of Environmental Science and Health Part A*. doi: 10.1080/10934529.2021.1895591.

Nazaroff, W. W. & Alvarez-Cohen, L. 2001 *Environmental Engineering Science*. Wiley, New York.

Oliveira, M., Araújo, A., Azevedo, G., Pereira, M. F. R., Neves, I. C. & Machado, A. V. 2015 Kinetic and equilibrium studies of phosphorous adsorption: effect of physical and chemical properties of adsorption agent. *Ecological Engineering* **82**, 527–530.

Panagiotou, E., Kafa, N., Koutsokeras, L., Kouis, P., Nikolaou, P., Constantinides, G. & Vyrides, I. 2018 Turning calcined waste egg shells and wastewater to Brushite: phosphorus adsorption from aqua media and anaerobic sludge leach water. *Journal of Cleaner Production* **178**, 419–428. https://doi.org/10.1016/j.jclepro.2018.01.014

Paradelo, A. R., Conde-Cid, M., Cutillas-Barreiro, L., Arias-Estéves, M., Nóvoa-Munoz, J. C., Álvarez-Rodrígues, E., Fernández-Sanjuro M, J. & Núnez-Delgado, A. 2016 Phosphorus removal from wastewater using mussel shell: investigation on retention mechanisms. *Ecological Engineering* **97**, 558–566. doi: 10.1016/j.ecoleng.2016.10.066.

Peng, L., Dai, H., Wu, Y., Peng, Y. & Lu, X. 2018 A comprehensive review of phosphorus recovery from wastewater by crystallization processes. *Chemosphere* **197**, 768–781. https://doi.org/10.1016/j.chemosphere.2018.01.098

Quina, M. J., Soares, M. A. R. & Quinta-Ferreira, R. 2017 Applications of industrial eggshell as a valuable anthropogenic resource. *Resource Conservation and Recycling.* **123**, 176–186. doi: 10.1016/j.resconrec.2016.09.027.

Ribeiro, I. C. A., Teodoro, J. C., Guilherme, L. R. G. & Melo, L. C. A. 2020 Hydroxyl-eggshell: a novel eggshell byproduct highly effective to recover phosphorus from aqueous solution. *Journal of Cleaner Production* **274**, 3–9. doi:10.1016/j.jclepro.2020.123042.

Rodrigues, A. S. & Ávila, S. G. 2017 Caracterização físico-química da casca de ovo de galinha e utilização como fonte para produção de compostos de cálcio. (Chicken eggshell physico-chemical characterization and use as a source for calcium compounds). *Revista Virtual de Química* **9** (2), 596–607. doi: 10.21577/1984-6835.20170035.

Snoeyink, V. & Jenkins, D. 1980 *Water Chemistry*. Wiley, New York.

Torit, J. & Phihusut, D. 2018 Phosphorus removal from wastewater using eggshell ash. *Environmental Science and Pollution Research* **26**, 34101–34109. doi:10.1007/s11356-018-3305-3.

U.S. Department of Interior & U.S. Geological Survey 2019 *Mineral Commodity Summaries 2019: Phosphorus*. Available from: https://s3-us-west-2.amazonaws.com/prd-wret/assets/palladium/production/mineral-pubs/phosphate-rock/mcs-2018-phosp.pdf (accessed 26 February 2020).

Van Vuuren, D. P., Bouwman, A. F. & Beusen, A. H. W. 2010 Phosphorus demand for the 1970–2100 period: a scenario analysis of resource depletion. *Global Environmental Change* **20** (3), 428–439. https://doi.org/10.1016/j.gloenvcha.2010.04.004

Wilfert, P., Kumar, P. S., Korving, L., Witkamp, G. J. & Van Loosdrecht, M. C. M. 2015 The relevance of phosphorus and iron chemistry to the recovery of phosphorus from wastewater: a review. *Environmental Science and Technology* **49** (16), 9400–9414. https://doi.org/10.1021/acs.est.5b00150

Yuan, Z., Pratt, S. & Batstone, D. J. 2012 Phosphorus recovery from wastewater through microbial processes. *Current Opinion in Biotechnology* **23** (6), 878–883. https://doi.org/10.1016/j.copbio.2012.08.001

First received 14 January 2021; accepted in revised form 21 June 2021. Available online 5 July 2021